Electronic Supplementary Information

Computational Design of Tetrazolate-based Metal–Organic Frameworks for CH$_4$ Storage

Xuanjun Wu[*,a]*, Liang Peng*[a]*, SiChen Xiang*[a] *and Weiquan Cai*[‡,*,b,a]

[a]School of Chemistry, Chemical Engineering & Life Sciences, Wuhan University of Technology, Wuhan 430070, P.R. China; [b]School of Chemistry and Chemical Engineering, Guangzhou University, Guangzhou 510006, P.R. China.

Table of Contents
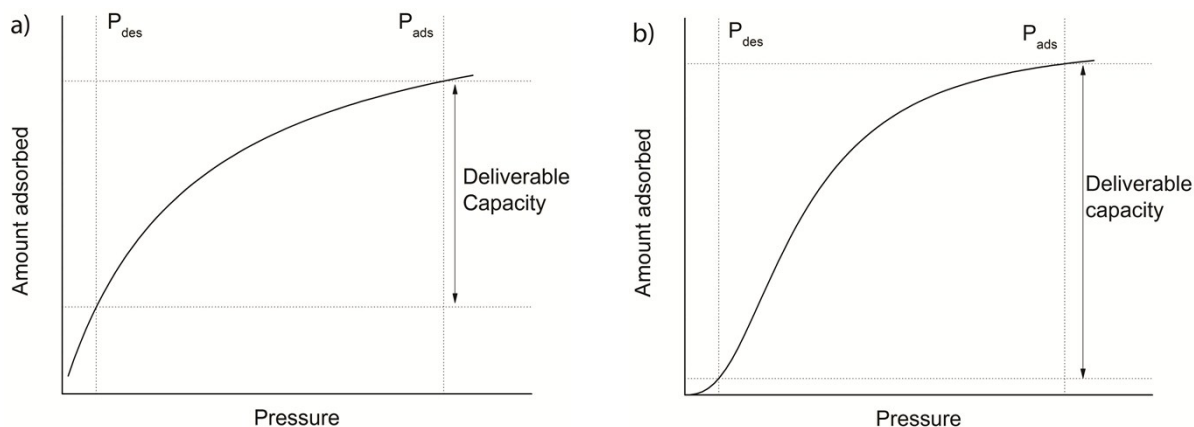
Deliverable capacity

Figure S1. Definition and comparison of deliverable capacity in porous adsorbents with different adsorption isotherms (a) Langmuir (b) S-shaped or stepped.

The deliverable capacity (DC) between charge and discharge pressures is considered as a key target to determine the performance of adsorbed natural gas (ANG) system. As illustrated in Figure S1a, if the adsorption isotherm of methane in a nanoporous material is a Langmuir type, the delivery capacity is usually not sufficiently high needed for a commercially viable ANG system.[1] Ideal nanoporous material usually presents an S-shaped isotherm (Figure S1b) or a gate-opening effect at high pressure.[1] The ultimate objective is that a high density of CH_4 is achieved at charge pressure and almost completely released at discharge pressure, thus boosting DC.
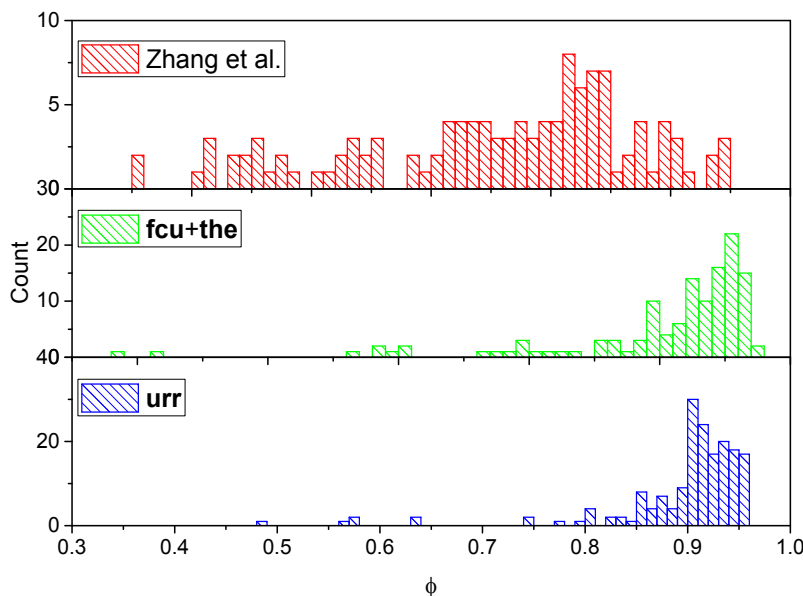
Geometrical characteristics

Figure S2. Void fraction histograms of 424 MOFs.

Figure S2 shows the void fraction histograms of 424 MOFs. The 120 MOFs designed by Zhang et al.[2] have a relatively more uniform distribution due to their topological diversity and short linkers. The **fcu-** and **the-**MOFs exhibit a peak at 0.98. Most of the **urr-**MOFs possess a peak at 0.90 ~ 0.98.
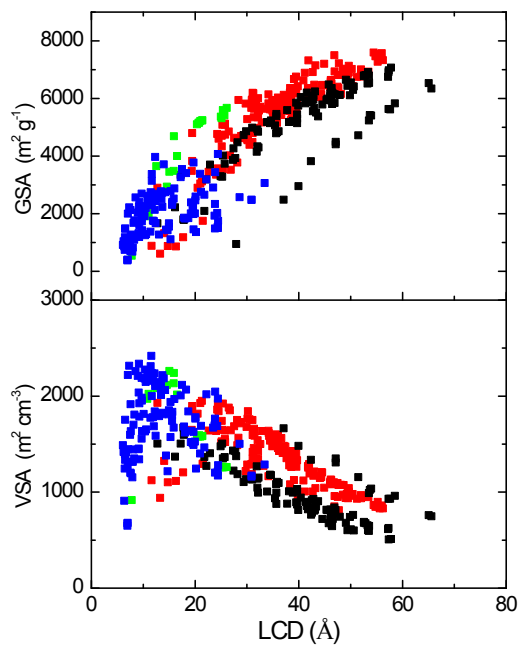

Figure S3. Gravimetric surface area (GSA) and volumetric surface area (VSA) versus the largest cavity diameter (LCD). Green, black and red: **fcu**, **the** and **urr** topologies. Blue: 120 MOFs by Zhang et al.[2]

Figure S3 illustrates the surface areas versus LCD. Approximately, the gravimetric surface area (GSA) has a linear relationship with the LCD; however, for the volumetric surface area (VSA), there is a maximum when LCD is in the range of 10-15 Å. Similar trend was observed in others MOFs[3,4] and porous polymer networks.[5]

Potential parameters

Table S1. Lennard-Jones potential parameters.

Atom type	ε/k_B (K)	σ (Å)
Zr	34.751	2.783
H	22.160	2.571
C	52.882	3.431
N	34.571	3.266
O	30.128	3.118
Cu	2.516	3.114
Zn	62.399	2.462
Co	7.045	2.559
CH_4	148.0	3.730

The interactions between framework atoms and CH_4 were represented by Lennard-Jones (LJ) potential with no consideration of coulomb interaction (equation S1), and cross LJ parameters were estimated by the Lorentz-Berthelot combining rules. All potential parameters are listed in Table S1 according to UFF [6] and TraPPE [7] force field.

$$U_{ij} = 4\varepsilon_{ij} \left[\left(\frac{\sigma_{ij}}{r_{ij}} \right)^{12} - \left(\frac{\sigma_{ij}}{r_{ij}} \right)^{6} \right] \quad (S1)$$

where i and j are interacting atoms, and r_{ij} is the distance between atoms i and j. ε_{ij} and σ_{ij} are LJ well depth and atomic pair equilibrium distance, respectively.
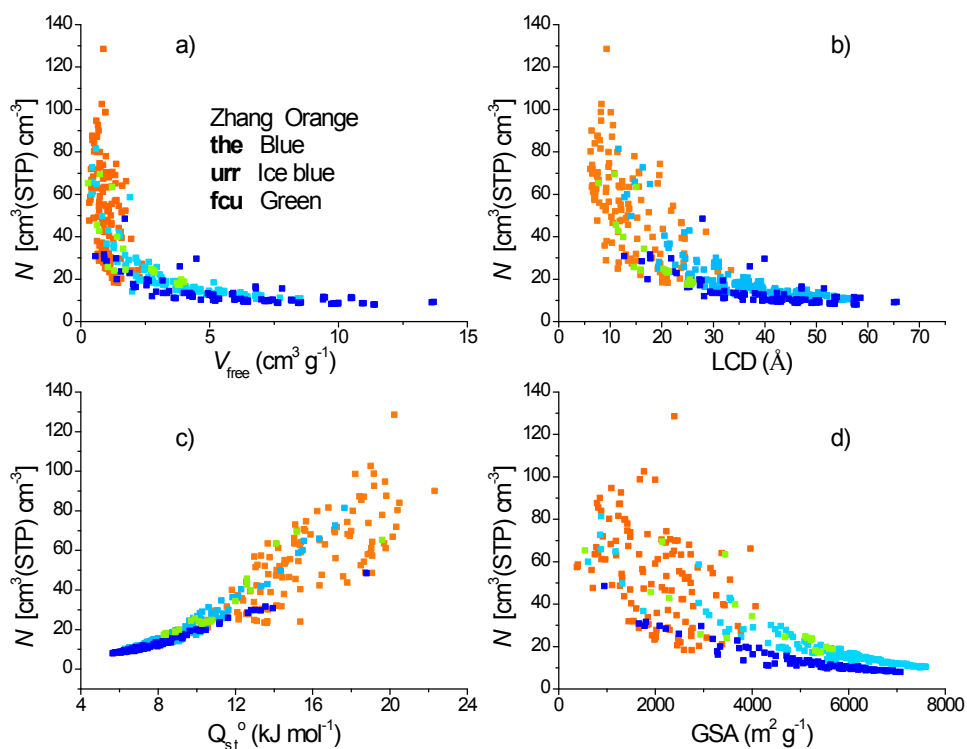
CH$_4$ uptake at 298 K and 5.8 bar

Figure S4. CH$_4$ uptake versus (a) free volume; (b) largest cavity diameter (c) isosteric heat (d) gravimetric surface area at 298 K and 5.8 bar.

There may be a ceiling of absolute methane storage capacity in porous frameworks at charge pressure according to recent research from different groups worldwide.[8-10] Chen et al.[10] even proposed a low-temperature strategy to boost the storage mileage of vehicle natural gas storage system in spite of its extra energy consumption. In other side, reducing NG storage capacity at delivery pressure could also achieve the enhancement effect for DC in the case of guaranteeing enough charging capacity. Therefore, it is significantly important to understand the relationship between absolute methane storage capacity at discharge pressure and structural properties of porous framework materials. Figure S4 shows the plots between CH$_4$ uptake at 5.8 bar and various structural properties of all designed materials. CH$_4$ uptake drops with increasing of free volume, LCD and gravimetric surface area (*GSA*) but rises with Q_{st}^o. At a high Q_{st}^o, the framework-CH$_4$ interaction is too strong and CH$_4$ adsorbed is not easy to desorb at delivery pressure, resulting in a lower deliverable capacity.

Top MOFs

The top 1 MOF is Zr-fcu-MOF-2Py with a predicted CH_4 deliverable capacity of 177 cm^3 (STP) cm^{-3} between 65 and 5.8 bar. Other top MOFs are in Figures S5. Those MOFs named with the beginning of "Zr-MOF-" were newly constructed by this work, while the others named with the beginning of "MOF-" were built by Zhang et al. Figures S6 illustrates methane adsorption isotherms in the top MOFs at 298 K.
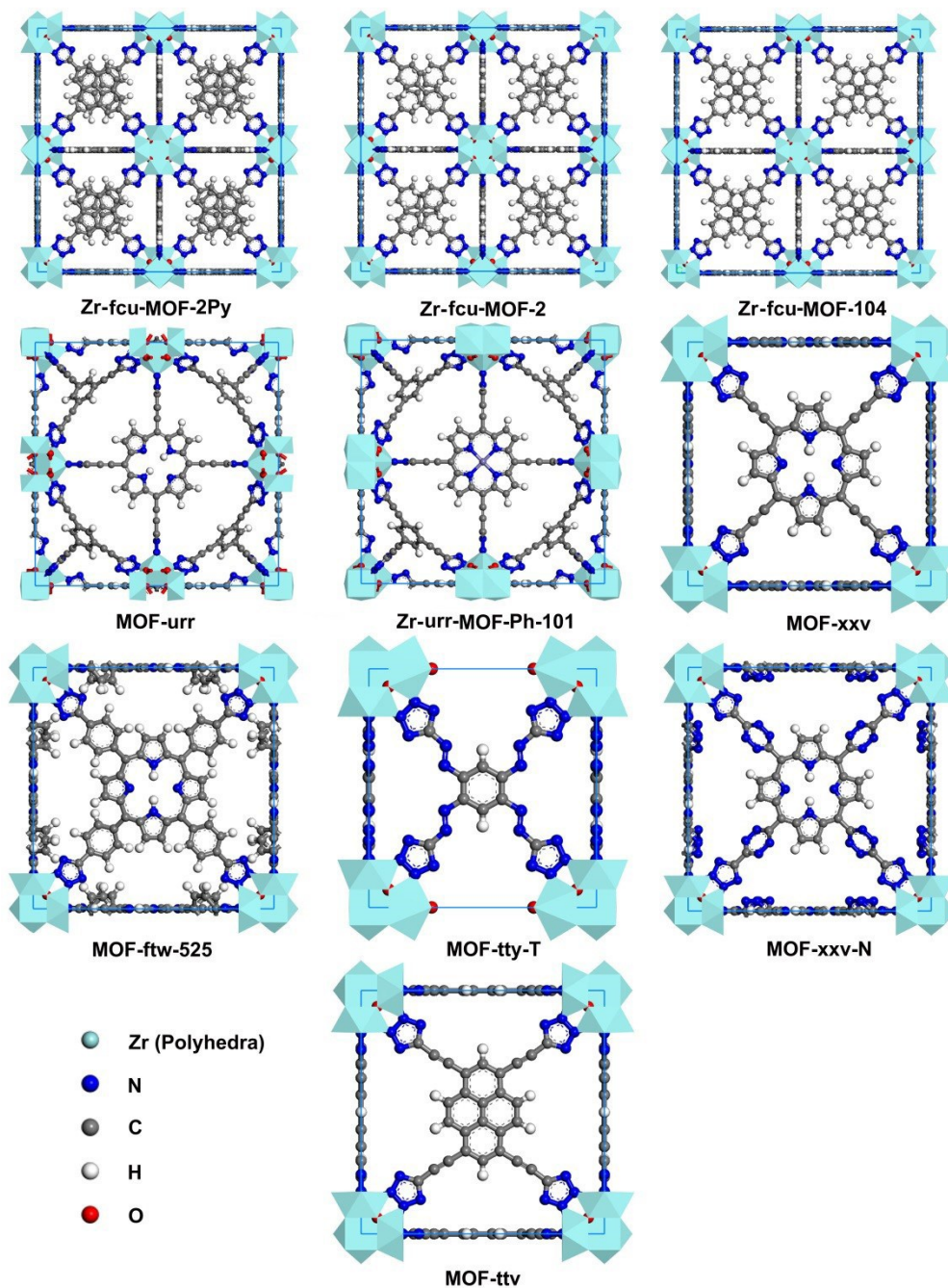

Figure S5. Top MOFs with excellent performance of methane delivery capacity.
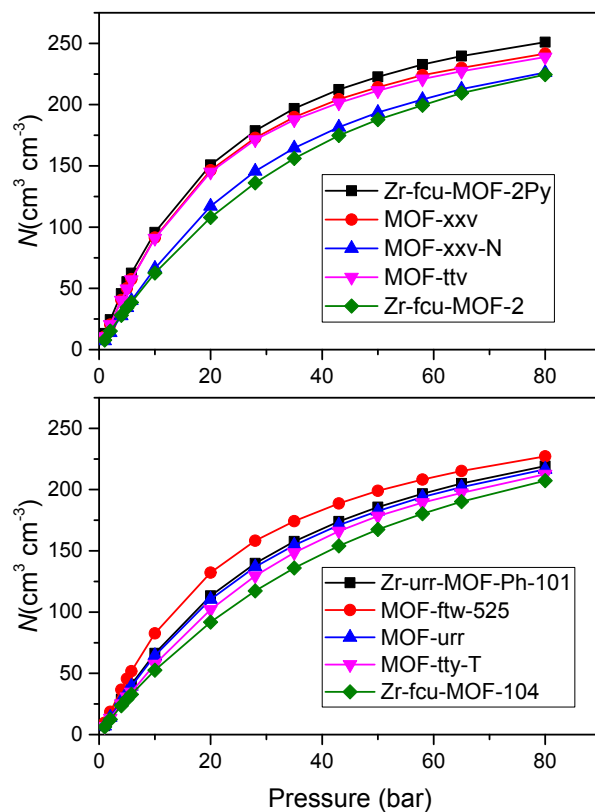
Figure S6. Adsorption isotherms at 298 K in top MOFs.

Radial distribution function

Radial distribution function $g(r)$ is commonly used to characterize structural ordering for multi-body system. The radial distribution functions $g(r)$ for atomic pairs between framework atoms in MOFs and methane molecules were calculated by using RASPA package according to the following equation:

$$g_{ij}(r) = \frac{\Delta N_{ij} \cdot V}{4\pi r^2 \cdot \Delta r \cdot N_i \cdot N_j} \qquad (S2)$$

where r is the distance between the geometric centres-of-mass of the atomic pairs i and j, ΔN_{ij} is the number of pairs j around i within a shell from r to $r + \Delta r$, V is the system volume, and N_i and N_j are the numbers of pairs i and j, respectively. Essentially, $g(r)$ gives the ratio of local density at position r to the

averaged density in the system. Figures S7 illustrates radial distribution functions between the framework atoms in Zr-fcu-MOF-2Py and CH_4 at 65 bar and 298 K. C-CH_4 and H-CH_4 atomic pair stronger interaction peaks are observed in agreement with the fact that there are two preferential adsorption sites of methane in Zr-fcu-MOF-2Py as seen in Figure 10.
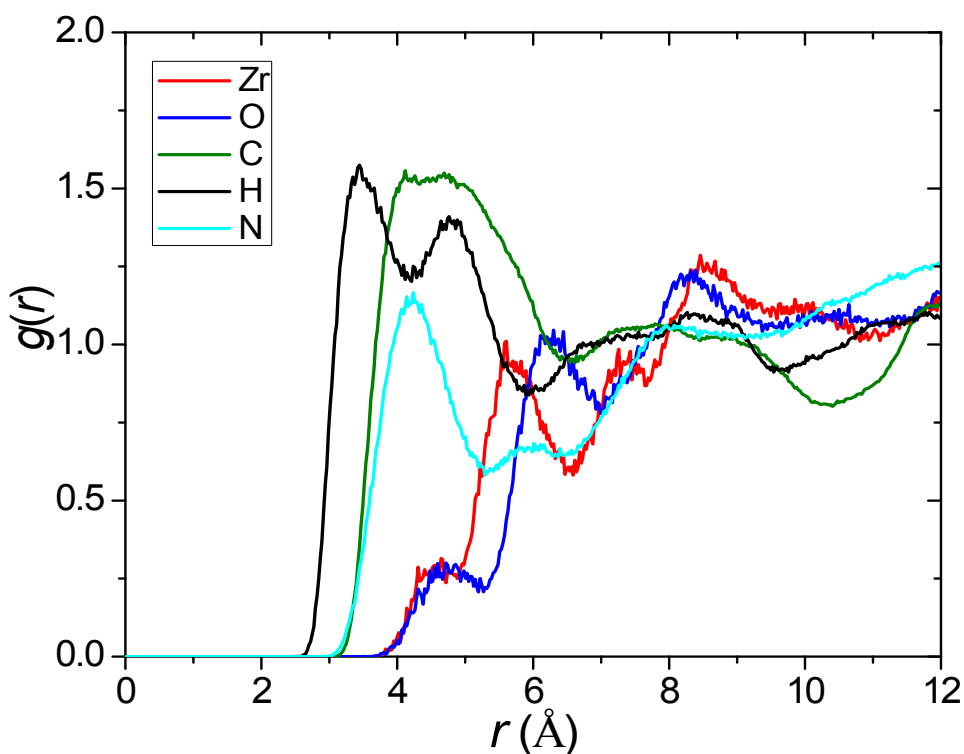

Figure S7. Radial distribution functions between the framework atoms in Zr-fcu-MOF-2Py and CH_4 at 65 bar and 298 K.

References

(1) Mason, J. A.; Oktawiec, J.; Taylor, M. K.; Hudson, M. R.; Rodriguez, J.; Bachman, J. E.; Gonzalez, M. I.; Cervellino, A.; Guagliardi, A.; Brown, C. M.; Llewellyn, P. L.; Masciocchi, N.; Long, J. R. Methane Storage in Flexible Metal-Organic Frameworks with Intrinsic Thermal Management. *Nature* **2015**, *527*, 357-361.

(2) Zhang, K.; Qiao, Z. W.; Jiang, J. W. Molecular Design of Zirconium Tetrazolate Metal–Organic Frameworks for CO_2 Capture. *Crystal Growth Design*, **2017**, 17, 543-549.

(3) Gómez-Gualdrón, D. A.; Wilmer, C. E.; Farha, O. K.; Hupp, J. T.; Snurr, R. Q. Exploring the Limits of Methane Storage and Delivery in Nanoporous Materials. *J. Phys. Chem. C* **2014**, *118*, 6941-6951.

(4) Gomez-Gualdron, D. A.; Colon, Y. J.; Zhang, X.; Wang, T. C.; Chen, Y.-S.; Hupp, J. T.; Yildirim, T.; Farha, O. K.; Zhang, J.; Snurr, R. Q. Evaluating Topologically Diverse Metal-Organic Frameworks for Cryo-Adsorbed Hydrogen Storage. *Energy Environ. Sci.* **2016**, *9*, 3279-3289.

(5) Martin, R. L.; Simon, C. M.; Smit, B.; Haranczyk, M. In Silico Design of Porous Polymer Networks: High-Throughput Screening for Methane Storage Materials. *J. Am. Chem. Soc.* **2014**, *136*, 5006-5022.

(6) Rappé, A. K.; Casewit, C. J.; Colwell, K. S.; Goddard, W. A.; Skiff, W. M. UFF, a Full Periodic Table Force Field for Molecular Mechanics and Molecular Dynamics Simulations. *J. Am. Chem. Soc.* **1992**, *114*, 10024-10035.

(7) Martin, M. G.; Siepmann, J. I. Transferable Potentials for Phase Equilibria. 1. United-Atom Description of N-Alkanes. *J. Phys. Chem. B* **1998**, *102*, 2569-2577.

(8) Simon, C. M.; Kim, J.; Gomez-Gualdron, D. A.; Camp, J. S.; Chung, Y. G.; Martin, R. L.; Mercado, R.; Deem, M. W.; Gunter, D.; Haranczyk, M.; Sholl, D. S.; Snurr, R. Q.; Smit, B. The Materials Genome in Action: Identifying the Performance Limits for Methane Storage. *Energy Environ. Sci.* **2015**, *8*, 1190-1199.

(9) Gomez-Gualdron, D. A.; Simon, C. M.; Lassman, W.; Chen, D.; Martin, R. L.; Haranczyk, M.; Farha, O. K.; Smit, B.; Snurr, R. Q. Impact of the Strength and Spatial Distribution of Adsorption Sites on Methane Deliverable Capacity in Nanoporous Materials. *Chem. Eng. Sci.* **2017**, *159*, 18-30.

(10) Li, B.; Wen, H. M.; Zhou, W.; Xu, J.; & Chen, B. Porous metal-organic frameworks: promising materials for methane storage. *Chem*, **2016**, 1(4), 557-580.